Applicability of Artificial Neural Network for Automatic Crop Type Classification on UAV-Based Images

*Ajayi O. G., Opaluwa Y. D., Ashi J. & Zikirullahi W. M.
Department of Surveying and Geoinformatics, Federal University of Technology, Minna
*Corresponding author: ogbajayi@gmail.com, gbenga.ajayi@futminna.edu.ng
ORCID*: http://orcid.org/0000-0002-9467-3569

_____

Recent advances in optical remote sensing, especially with the development of machine learning models have made it possible to automatically classify different crop types based on their unique spectral characteristics. In this article, a simple feed-forward artificial neural network (ANN) was implemented for the automatic classification of various crop types. A DJI Mavic air drone was used to simultaneously collect about 549 images of a mixed-crop farmland belonging to Federal University of Technology Minna, Nigeria. The images were annotated and the ANN algorithm was implemented using custom-designed Python programming scripts with libraries such as NumPy, Label box, and Segmentation Mask, for the classification. The algorithm was designed to automatically classify maize, rice, soya beans, groundnut, yam and a non-crop feature into different land spectral classes. The model training performance, using 70% of the dataset, shows that the loss curve flattened down with minimal over-fitting, showing that the model was improving as it trained. Finally, the accuracy of the automatic crop-type classification was evaluated with the aid of the recorded loss function and confusion matrix, and the result shows that the implemented ANN gave an overall training classification accuracy of 87.7% from the model and an overall accuracy of 0.9393 as computed from the confusion matrix, which attests to the robustness of ANN when implemented on high-resolution image data for automatic classification of crop types in a mixed farmland. The overall accuracy, including the user accuracy, proved that only a few images were incorrectly classified, which demonstrated that the errors of omission and commission were minimal.

Keywords: Artificial Neural Network (ANN), automatic crop-type classification, image segmentation, image annotation, precision agriculture

INTRODUCTION

The basic distinction between vegetated and non-vegetated regions, or woodland and open fields, is vegetation classification (Timalsina *et al*., 2021). In certain cases, such distinctions can be quite important, especially when data is pooled across broad areas or monitored over lengthy periods of time. An ecosystem of plant is a group of plants that have joint interdependencies with one another and with their surroundings (Horn *et al*., 2017). Crop classification is by far the most essential aspect of the vegetation classification because in several settings, agricultural crops are frequently inspected and cultivated in regular regional fields with a specific crop per field (Mengist, 2019).

In precision agriculture, remote sensing techniques integrated with machine learning algorithms can be used in the classification of several classes of crops (Mekonnen *et al*., 2019). It has the potential to be significantly faster, more precise, and hence, less expensive than traditional approaches for estimating regional crop area (Nitze *et al*., 2012). Crop type data at the field level can be utilized for agricultural surveys, subsidy

control, or as a supplement to crop yield forecasting and shortages. Crop classification is determined by a crop's spectral response pattern and image texture pertaining to a particular crop (Murmu & Biswas, 2015). For correct crop identification, it is vital to understand the phases of growth of each crop because crop properties fluctuate throughout the growing season (Pang *et al*., 2020), hence, satellite images taken at various times throughout the growth cycle are frequently useful (Seelan *et al*., 2003).

The concept of artificial intelligence in image classification and automatic feature identification and extraction is developing and becoming an important method in a variety of disciplines (Fielding & Zhang, 2018; Ajayi & Oruma, 2022; Ajayi & Ojima, 2022). Without this technique, the notion of human anatomy and the digital approach to monitoring human interior structures is becoming unachievable in the medical industry. In remote sensing, image classification is a strategy of categorizing diverse picture components into several geographical spectral classes belonging to the same class (Li *et al*., 2014). This is a technique of image processing that entails classifying and segmenting multiple visual parts with comparable attributes (Wisniewski & Schowengerdt, 2005). Because of the success of a number of commercial applications that utilizes this technology, Artificial Neural Networks (ANN) and other machine learning methodologies have garnered considerable attention. Consequently, relatively robust open source frameworks and solutions have been established, bringing this technology to the attention of ordinary developers and users (Sootla & Matiisen, 2015).

LITERATURE REVIEW

Remote sensing relies heavily on image classification (Cui *et al*., 2015; Xu *et al*., 2016; Liu *et al*., 2018; Pham *et al*., 2018)

which results in the production of thematic maps. The method of making thematic maps using satellite images is known as thematic mapping (Foody, 2002). A thematic map is a data-driven visual representation that depicts the spatial distribution of a certain subject (Hamzah, 2015). Vegetation types, such as trees, crops, and grasslands, are examples of themes. Within a subject, finer sub-themes can be created to refine the classification process, such as identifying trees as deciduous or evergreen. To classify images, spectral discreteness of categories/classes or spectro-temporal variation is generally utilized (Ashish *et al*., 2009).

The majority of land-use intensity classifications have a specific distribution which is used to generate spectral classifications based on image categorization. Within a given geographical range, the spatiotemporal configuration of these reflectance values might reveal important information towards categorizing the images (Fung & Chan, 1994). The texture information in a picture may also be used to classify it. Several factors for texture identification in images have been presented by Maillard (2003), Ehsanirad & Yh (2010), Lee *et al*. (2016), Shaha and Pawar (2018) and Zhang *et al*. (2019). Some of these include contrast, inverted difference moment, correlation, entropy, etc.

The homogeneity of the image is determined by the angular second moment. On the other hand, the degree of local variation contained in a picture is measured by contrast (Yang *et al*., 2012) while the gray-tone linear-dependencies in a picture are measured through correlation (Simonthomas *et al*., 2014). Also, the level of local similarity is measured by the inverse difference moment (Zhao & Qin, 2018) while the entropy of a gray tone co-occurrence in a picture is a measure of its average uncertainty (Hendrawan *et al*., 2019). Image categorization and analysis have traditionally relied on the contrast

factor, the entropy factor, the angular second moment factor, and the inverted difference moment factor.

Classification accuracy is decreased by higher variability (Maniruzzaman *et al*., 2018; Dhingra & Kumar, 2019). The majority of land-use classification research has previously centred on multispectral image analysis (Tehrany *et al*., 2014; Hassan *et al*., 2016; Huang *et al*., 2018). Gray-scale pictures have been used in quite a few situations (Zauner *et al*., 2014; Kasim *et al*., 2017), and no comparisons to multispectral data processing have been done. Because of the little spectral information available in these pictures, accurate categorization of grey-scale photos into distinct land-uses has proved to be increasingly difficult (Ashish *et al*., 2004). Several novel methodologies have outperformed classical approaches, such as those of the contextual classification scheme and techniques centred on fuzzy sets or with their permutations (Blaschke *et al*., 2004). Contextual classification algorithm enhance the level of complexity of information collected by adding extra bands once contextual information is available in some fashion, or they presume the occurrence of local attributes specified in such a region in which geographic dependency seems to be significant. ANNs harness the brain's processing to create algorithms that may be used to model complicated patterns and anticipate outcomes (Salyut & Kurnaz, 2018). There are billions of neurons in our brain that process information in the form of electric impulses.

ANN is a computationally analytical model that is based on biological learning analogies, and mimics a few of the recognized properties of biological neural systems (Mocanu *et al*., 2018). It is a network of interrelated processing components which functions similarly to neurons (Maind & Wankar, 2014). These processing units are linked by connection weights, which are akin to neurotransmitters in the human cerebral cortex. Supervised learning is frequently achieved in an ANN via training or exposure to a typically known collection of set of data (Ashish *et al*., 2009). The connection weights are adjusted by the training algorithm in an iterative method that minimizes the error (Ding *et al*., 2015).

Previous researches have demonstrated the advantages of ANN over several traditional statistical approaches in a variety of issues, including classification challenges (Heng *et al*., 2009; Wei *et al*., 2018; Ahmad *et al*., 2020; Zohdi *et al*., 2022). It is also frequently employed during automatic data classification and segmentation, and it has been suggested especially for issues involving a great deal of data variability (Moshou, 2001; Mehdy *et al*., 2017; Mohammed *et al*., 2017). Benediktsson *et al*. (1990) demonstrated the practicality of using ANNs to classify the land use of remotely sensed picture regions. The neural network classifier approach was compared with normal empirical classification methods (Foody & Zhang, 2001; Galbraith *et al*., 2012). The per-pixel method was described in these works as one of the numerous categorization algorithms based on ANNs (Agrawal & Bawane, 2015). Because the geographic diversity of ground characteristics rises as spatial resolution increases, the per-pixel technique is likewise ineffective for classifying high resolution pictures (Hussain *et al*., 2013).

Various researchers opined that using ANN for image classification yields high level of accuracy (Tsai, 2002; Rashmi & Mandar, 2011; Thai *et al*., 2012; Mahmon & Ya'acob, 2014). While ANN has been used for the classification of different land features, there are significantly sparse evidences of its robustness in automatic crop type classification using Unmanned Aerial Vehicle (UAV) acquired images, a gap this study aims to fill. The purpose of

this study is to build and train an artificial neural network that can classify various crop varieties in a mixed farm from UAV acquired images with a view to achieving a potentially much faster, more accurate and therefore, more cost effective means of classification than the conventional methods of generating regional crop area estimates.

MATERIALS AND METHODS

The study area adopted for this study is the agricultural mixed farmland belonging to the Federal University of Technology Minna, located at Garatu area of Minna in Niger State. It covers an area of 21 hectares and it is geographically located between Lon: $6^0 25'22.4"$, Lat: $9^0 32'3.8"$ and Lon: $24^0 17'59.8"$, Lat: $9^0 8'29.8"$. The plots are mainly composed of loamy soil, and cultivation is done only in the raining season, and with mixed cultivation practices. A geographic description of the study area is presented in Figure 1.
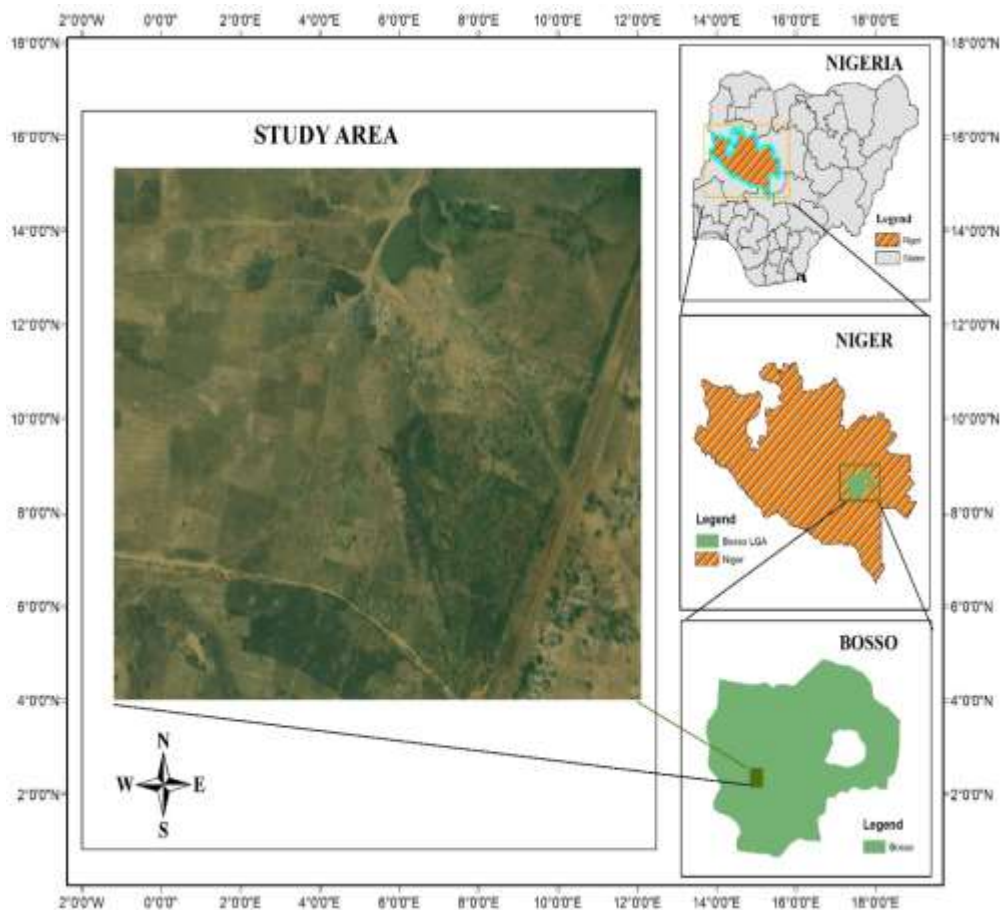

Figure 1: Study area

Data Collection

Spatial coordinates of the ground control points were collected with the aid of two (2) differential global positioning system (DGPS) receivers. The ground truth data (spatial coordinates) acquired with the DGPS receivers to measure the centre of the pre-marked Ground Control Point (GCP) markers were utilized as reference data for the UAV acquired images. About 549 overlapping image pairs of the

farmland were captured using a DJI Mavic air drone on 20th June 2019. This UAV is a plastic built vertical take-off and landing vehicle. To start the UAV's propellers and initiate take-offs and landings, a remote control was utilized. The remainder of the trip was conducted using the GPS waypoints for autonomous navigation. The drone is equipped with a battery capacity of 2970mAh, and a Red Green Blue (RGB) sensor with a 4:3 4056 x 3040 and 16:9 4056 x 2280 (12MP) pixel detector, and it was deployed at a height of 60 meters above ground level, with an angular FOV of 850 which gave 0.019 m•pixel^{-1} resolution (DJI Mavic Air, 2022). The classification was performed on the 549 acquired and annotated image pairs. Figure 2 shows the workflow describing the step-by-step procedure adopted in the development of the automatic crop type classification scheme.
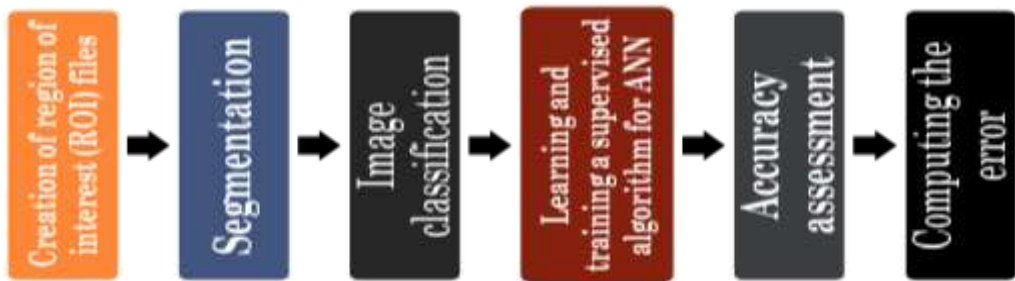
Figure 2: An overview of the methodological workflow

Data Processing

Hp elitebook Intel Core i5-432OU, central processing unit of 2.0GHz, 8GB RAM with 64 bit Operating System and along with the following software packages; Python programming, NumPy, Label box, and Segmentation Mask, were used. The network took an average of 223 minutes to complete the computation. One ROI file was used to train the system, while the other served as a testing dataset. Out of the 549 annotated photos, the neural network was trained using 70% of the data, and the network was tested with the remaining 30%.

In order to automatically classify the crop types using ANN, the photos were loaded sequentially from the file directory. After that, the file was extracted to obtain a list of all image file names, which was followed by its importation into the Keras library. Keras is a deep learning API for creating neural networks at a high level. It was used to make the implementation

of the neural network easy. To make the whole image vector and picture ID 64 by 64 in size, a target size vector was set. This was done because, with the exception of vectors, neural networks function with multi-dimensional arrays. There were a total number of 549 images by 4096 columns. After that, label encoding was employed to transform images to numbers, which were then translated into classes. The classes were subsequently converted to columns using one-hot encoding.

Six different classes were labelled using RGB segmentation masks with label boxes in this segment. It labelled the classes with each of them, as well as their segmentation, and then used an image segmentation mask to segment each type of crop on every single image. After building the network, the entire dataset was grouped into two (2) selected sample classes; the training sample and the test sample. The training sample was then utilized to train the network which

subjected it to a learning process, while the test sample was used to assess the classifier's accuracy. Various methods, such as the hold-out technique, cross validation, and random sampling and so on can be used to divide or group a data set. For this study, cross-validation which is a data resampling technique that is used to evaluate the generalization capabilities of prediction models and to avoid over-fitting was deployed. The learning phases of a neural network are described as follows:

1. The input, output, and hidden layer networks were specified by a set number of nodes.

2. For the learning process, a simple feed-forward neural network method was utilized because it does not require a user-specified problem-solving technique (as seems to be the case with classical coding) and would instead "learn" from examples in the same way that people do. It also has a natural propensity to generalize. This implies that it is capable of recognizing and responding appropriately to sequences that are comparable but not identical to those it has already been taught to detect (Benardos & Vosniakos, 2007).

During the neural network's training, the recorded error was initially analyzed and the weights were modified accordingly. Gradient descent and back propagation techniques were used to change the weights. To discover the direction and rate at which the parameters should be updated, gradient descent method was used. For the weights and bias parameters, the neural network class creates randomized start values. Although the weights and bias for a single data sample have indeed been adjusted, the aim is for the network to generalize over the whole set of data. ADALINE, otherwise known as stochastic gradient descent, is a method in which the model makes a projection based on randomly selecting a piece of training data,

evaluates the error, and then adjusts the variables at each iteration.

In the neural network, both the weights and the bias vectors need are supposed to be updated. Because the weights and bias are independent variables on which the function used to measure the error is based, they may be changed and adjusted to get the desired outcome. The network that was built includes four layers, and each layer does have its own set of functions, hence the network is interacting with function composition. This indicates that perhaps the error function remains np.square(x), however x has now become the outcome of a different function, so that the derivatives of the said error with respect to weights must be computed.

Error Estimation and Accuracy Assessment

The cost function, also known as the loss function, was used to calculate the error. The Mean Square Error (MSE) cost function was employed as a function for this study. The MSE was computed by first calculating the distinction between the target and thus the predictions, and then multiplying the outcome by itself. There is possibility that the network may produce the wrong decision by providing a value larger or lesser than that of the real number. The MSE provides a positive number in the end because it is the squared difference of both the forecast as well as actual outcome.

The confusion matrix was used to assess the accuracy of the categorization findings which is typically used in machine learning. The total error matrix (Table 1) is represented by the full confusion matrix, which is the combination of all classes with each other using the peer-to-peer approach, including all commission and omission errors for each class. The overall accuracy was first determined through adding the numbers of properly categorized crops by the sum total of crop values.

RESULTS AND DISCUSSION

The images were classified into five (5) classes of various crops such as maize, rice, beans, groundnut, yam and one (1) non-crop class. Few samples of the images are presented in the merged block of images shown in Figure 3. As at the time the aerial imageries were acquired, the farm had already been weeded.

On previously unknown data, the resultant artificial neural network had an accuracy of 87.7% after implementing all of the previously stated features. The neural network was trained using a learning rate of 0.001 and a momentum of 0 for 30 time steps (which is the amount of instances the complete dataset was passed through the network) and a batch size of 20 (the number of inputs which were delivered through the network just before weights were modified). The algorithm ended up taking the network 3hours 43 minutes to complete the entire training process. Furthermore, the model predicted and categorised the majority of the images based on their labels, and there is a predicted chance that the image belongs to that specific class for each label and class.
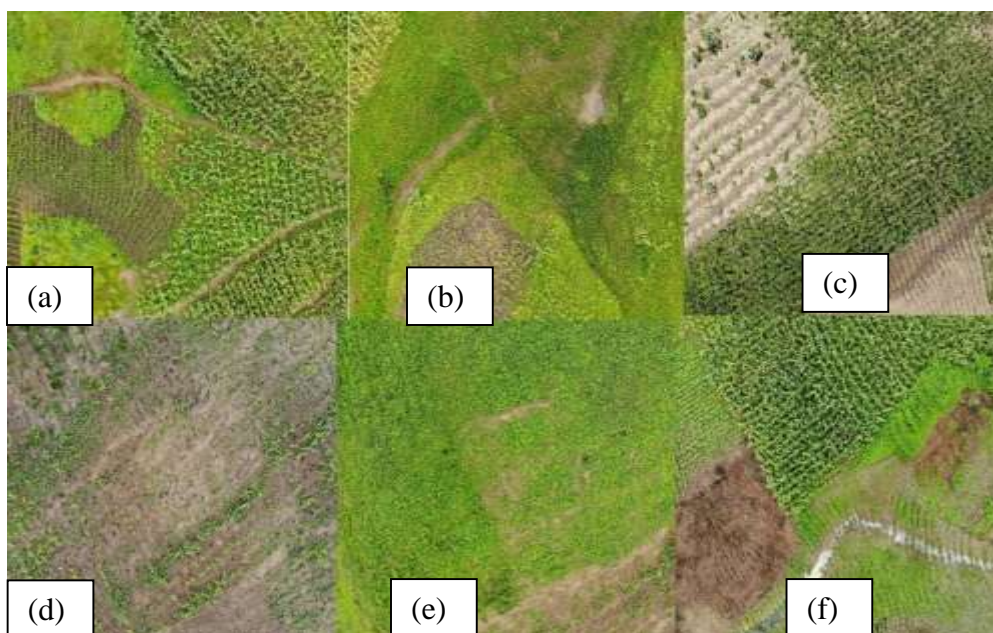
Figure 3: Image block consisting of samples of the different classes (a) The image comprises of maize and rice. (b) The image consist of beans crops. (c) The image consists of maize crops. (d) The image consists of partly maize crops and bare ground. (e) Consist of groundnuts. (f) Consist of maize and rice crops

The neural network has six levels; a single input and output layer, and four layers that are hidden, which represent different types of data sets. Figure 4 shows a graph of cumulative error for each of the four hidden layers, each with 100 neurons. In a nutshell, a randomized instance was chosen from the dataset, appropriate gradient was computed, as well as the weights and bias were subsequently modified. At every 100 iterations, the cumulative error was calculated and the results were stored in an array. The array was used to show how the error changed over time during training.

The graph in Figure 4 was created in the same directory as the IPython process of

which the process completes a list of all the attributes defined for deep learning. Following the highest decline, the error rapidly increases and decreases from one iteration to the next. Figure 4 presents a graph depicting the training error for a neural network instance. From the graph, it can be seen that the overall error is decreasing consistently as it goes down the iterations, even when it appears to be sinusoidal in nature. The training error peaked at the beginning of the iteration (greater than 3.75) but closed up to less than 1.0 at the end. This means that the network was able to extract features reliably.
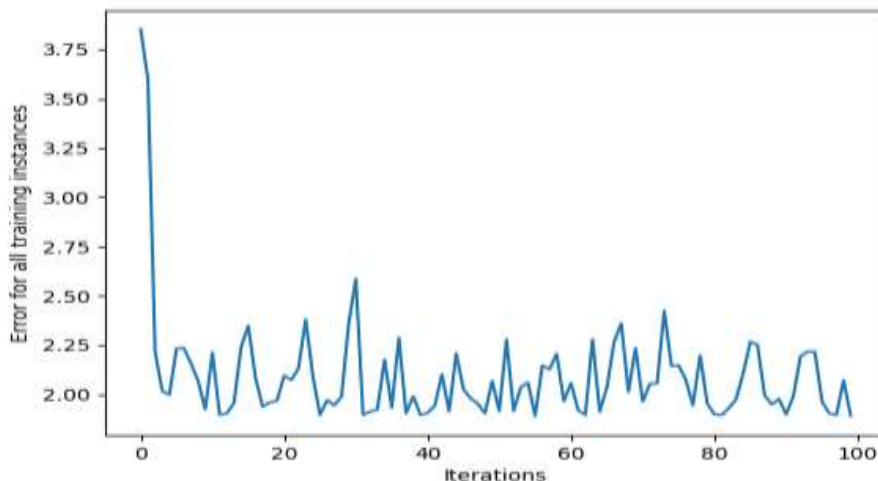
Figure 4: Cumulative training error over different iterations

Table 1 presents a confusion matrix depicting the accuracy of the automatic crop type classification. Column 1 of the table shows that there was only one groundnut sample in the entire dataset and the model correctly classified it as groundnut, which is a true positive. Also, the second column shows that 131 images were accurately classified as maize, which is also a true positive, 4 images were misclassified as rice, 1 misclassified as yam, and 2 images misclassified as bare ground, which are all false negatives. The algorithm accurately classified 10 images as rice and 2 images as maize (true positive). No image of soya beans was misclassified (true positive), six images were accurately classified as yam (true positive), and one image was misclassified as maize (false negative). There were no misclassifications in the five images that were correctly identified as barren ground (true positive).

Table 1: Confusion matrix of classified images

	Groundnut	Maize	Rice	Soya beans	Yam	Bare ground	Total
Groundnut	1	0	0	0	0	0	1
Maize	0	131	4	0	1	2	138
Rice	0	2	10	0	0	0	12
Soya beans	0	0	0	2	0	0	2
Yam	0	1	0	0	6	0	7
Bare ground	0	0	0	0	0	5	5
Total	1	134	14	2	7	7	165
Accuracy (%)	100	97	71	100	85	71	87

The automatic classification of the crop types using ANN provided a positive result, recognizing the majority of the crops while misclassifying a few, indicating that ANN is useful for multi-crop classification. However, if each class has an unequal amount of observations or the dataset includes well over two classes, classification accuracy itself might be deceptive or false, hence the need to explore other accuracy measures.

Overall accuracy from the confusion matrix $= \frac{155}{165} = 0.939393.$ (1)

User Accuracy

User accuracy is the probability that an item projected to belong to a given class really belongs to that class. The probability is computed by simply dividing the total number of values anticipated in a class by the number of

Overall Accuracy

The overall accuracy is estimated by adding the number of properly categorized crops and then dividing the properly categorized crops by the sum total of the crops. The accurately identified crop numbers may be found on the upper-left to lower-right diagonal of the confusion matrix.

Hence, correctly classified values: 1+131+10+2+6+5= 155

Sum total number of classified crop values = 165

successfully estimated parameters. The user accuracy result shows that Groundnut, Soya beans and bare ground classes were perfectly classified since their values are 1, followed by Maize, Yam and Rice, respectively (see Table 2).

Table 2: Estimated user accuracies

Classes	Probability
Groundnut	1.0000
Maize	0.9493
Rice	0.8333
Soya beans	1.0000
Yam	0.8571
Bare ground	1.0000

Errors of Omission

The proportion of values that belong to one class but were projected to belong to a different class is known as omission errors. They are metrics of ascertaining how many false negatives are there in a sample. Except for the values along the main diagonal, all omission errors are displayed in the confusion matrix's columns. Table 3 presents the error of omission for each of the six classes.

Table 3: Estimated errors of omission

Classes	Errors of omission
Groundnut	0
Maize	0.0224
Rice	0.2857
Soya beans	0
Yam	0.1429
Bare ground	0.2857

In Table 3, the first column (Groundnut) and the fourth column (Soya beans) yielded zero error of omission meaning there exist no omission error, followed by the second column (maize) with 0.022 error of omission, then columns five, three and six, in that order. This means that the classifier marked 2 points accurately (Groundnut and soya beans) and the class was actually correct.

Errors of Commission

The proportion of values that were anticipated to be in a class but are not really in that class is referred to as errors of commission. They are a measure of calculating how many false positives there are. Except for the diagonal values, commission errors are displayed in the rows of confusion matrix table. Computed errors of commission for each of the six classes are presented in Table 4.

Table 4: Estimated errors of commission

Classes	Errors of commission
Groundnut	0.0000
Maize	0.0507
Rice	0.0667
Soya beans	0.0000
Yam	0.1429
Bare ground	0.0000

The loss curve, also known as the log loss in Figure 5 displays the model's aim of decreasing the loss by assessing the performance of a classification model with a probability value output between 0 and 1. The goal of the training technique was to achieve minimal feasible loss. By dividing this same numbers of accurate training instances by the numbers of wrong training examples, the loss was calculated. Or, in the event of regression issues, how close it came to getting the right answer. Given a true observation (isDog = 1), the graph in Figure 5 depicts the range of probable loss levels (vertical plane) and the numbers of epochs on the horizontal plane. Log loss diminishes as the estimated probability approaches 1. The log loss, on the other hand, rapidly grows when the expected probability lowers. The loss curves were smoothing out, showing that the model was becoming better as it learned. Because the test loss and training loss are the same, the model does not over fit the training data.
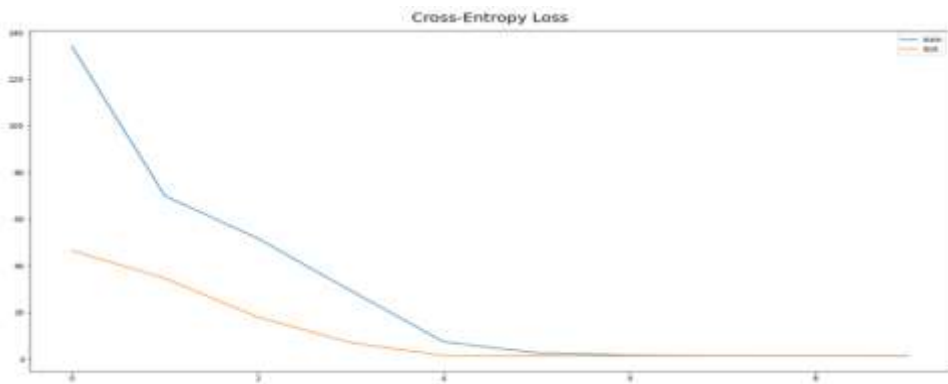
Figure 5: Cross entropy loss graph

The accuracy curve in Figure 6 demonstrates how the training and test accuracy differ. The training accuracy progressively grows while the test accuracy swiftly converges, according to the accuracy curve. The accuracy versus epoch curves for training and testing datasets finally converged towards each other. The vertical plane depicts the accuracy values on a scale of 0-1 while, the horizontal plane depicts the numbers of epochs. This also demonstrates that the model is not too fitted (no over-fitting).
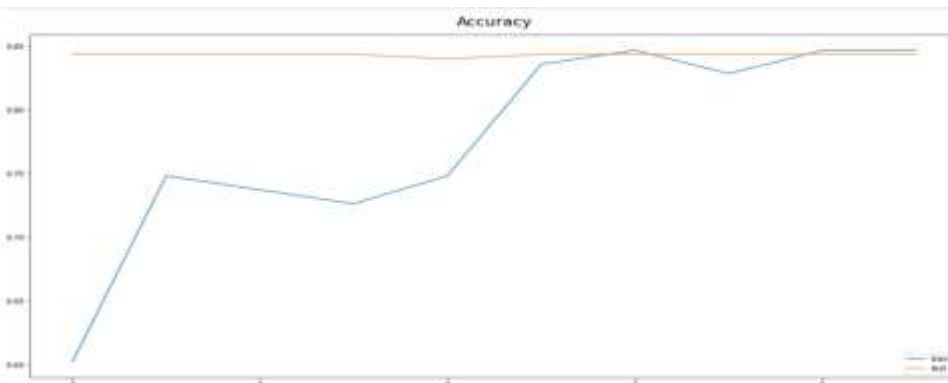
Figure 6: Accuracy curve of the network architecture

CONCLUSION

In this study, the details of the development of an artificial neural network (ANN) based system for automatic crop type classification was presented. The algorithm did not only carry out training and learning of the dataset, but also proved to be capable of automatically and accurately identifying and classifying the specific crop type using UAV image data which is very important for agricultural or farmland inventory, and in precision agriculture. The ANN consistently provided higher training classification accuracy, indicating that it is able to accurately characterise different class appearances. An average of 87.87% general accuracy was recorded throughout the categorization, indicating general consistency in the classification of crops into the six (6) separate groups. In addition, an overall classification accuracy of 0.9393 was attained during the automatic classification of the crop types. With a lower cumulative error, the model correctly predicted and identified majority of the images, as evident in the classification's confusion matrix. The overall accuracy, including user accuracy proved that only few images were incorrectly classified, which demonstrated that the errors of omission and commission were minimal. The loss curve also flattened down with minimal over-fitting, showing that the model was improving as it trained. Because the test loss and training loss are the same, the model does not over-fit the training data. The accuracy versus epoch curves for training and testing datasets finally converged towards each other. This also demonstrates that the model is not too fitted (no over-fitting). Further research effort will explore possible approaches of enhancing the developed artificial neural network. Firstly, the programs will be modified to make the overall implementation scheme more readable and efficient. Secondly, additional hidden layers will be added to the network to give it the abilities it needs to interpret increasingly complex data correlations. Furthermore, the applicability and efficiency of some other neural network architecture such as the convolutional neural network (CNN) in automatic crop type classification will be investigated and compared with the developed ANN model.

REFERENCES

Agrawal, R. K. & Bawane, N. G. (2015). Multi-objective PSO based adaption of neural network topology for pixel classification in satellite imagery. *Applied soft computing*, *28*, 217-225.

Ahmad, T., Zhang, H. & Yan, B. (2020). A review on renewable energy and electricity requirement forecasting models for smart grid and buildings. *Sustainable Cities and Society*, *55*, 102052.

Ajayi, O. G. & Ojima, A. (2022). Performance evaluation of selected cloud occlusion removal algorithms on remote sensing imagery. *Remote Sensing Applications: Society and Environment*. 25, 1-17. https://doi.org/10.1016/j.rsase.2022.100700

Ajayi, O. G. & Oruma, E. (2022). On the applicability of integrated UAV photogrammetry and automatic feature extraction for cadastral mapping. *Advances in Geodesy and Geoinformation (formerly Geodesy and Cartography).* 17 (1), https://doi.org/10.24425/gac.2022.141172

Ashish, D., Hoogenboom, G. & McClendon, R. W. (2004). Land-use classification of gray-scale aerial images using probabilistic neural networks. *Transactions of the ASAE*, *47*(5), 1813.

Ashish, D., McClendon, R. W. & Hoogenboom, G. (2009). Land-use classification of multispectral aerial images using artificial neural networks. *International Journal of Remote Sensing*, *30*(8), 1989-2004.

Benardos, P. G. & Vosniakos, G. C. (2007). Optimizing feedforward artificial neural network architecture. *Engineering applications of artificial intelligence*, *20*(3), 365-382.

Benediktsson, J. A., Swain, P. H. & Ersoy, O. K., (1990). Neural network approaches versus statistical methods in classification of multisource remote sensing data. *IEEE Trans. Geosci. Remote Sensing*, 28(4), 540-551.

Blaschke, T., Burnett, C. & Pekkarinen, A. (2004). Image segmentation methods for object-based analysis and classification. In *Remote sensing image analysis: Including the spatial domain* (pp. 211-236). Springer, Dordrecht.

Cui, S., Schwarz, G. & Datcu, M. (2015). Remote sensing image classification: No features, no clustering. *IEEE Journal of Selected Topics in Applied Earth Observations and Remote Sensing*, *8*(11), 5158-5170.

Dhingra, S. & Kumar, D. (2019). A review of remotely sensed satellite image classification. *International Journal of Electrical and Computer Engineering*, *9*(3), 1720.

Ding, S., Zhao, H., Zhang, Y., Xu, X. & Nie, R. (2015). Extreme learning machine: algorithm, theory and applications. *Artificial Intelligence Review*, *44*(1), 103-115.

DJI-Mavic Air (2022), United States, accessed 19 February 2022, < https://www.dji.com/mavic-air>

Ehsanirad, A. & Yh, S. K. (2010). Leaf recognition for plant classification using GLCM and PCA methods. *Oriental Journal of Computer Science and Technology*, *3*(1), 31-36.

Fielding, B. & Zhang, L. (2018). Evolving image classification architectures with enhanced particle swarm optimisation. *IEEE Access*, *6*, 68560-68575.

Foody, G. M. (2002). Status of land cover classification accuracy assessment. *Remote Sensing of Environment*, 80(1), 185-201.

Fung, T. & Chan, K., (1994). Spatial composition of spectral classes: a structural approach for image analysis of heterogeneous land-use and land-cover types. *Photogramm. Eng. Remote Sens.*, 60 (2), 173-180.

Galbraith, C. S., Merrill, G. B. & Kline, D. M. (2012). Are student evaluations of teaching effectiveness valid for measuring student learning outcomes in business related classes? A neural network and bayesian analyses. *Research in Higher Education*, *53*(3), 353-374.

Hamzah, N. A. (2015). *Land Use/land Cover Classification and Change Analysis by Multitemporal Remote Sensing Data* (Doctoral dissertation, UMP).

Hassan, Z., Shabbir, R., Ahmad, S. S., Malik, A. H., Aziz, N., Butt, A. & Erum, S. (2016). Dynamics of land use and land cover change (LULCC) using geospatial techniques: a case study of Islamabad Pakistan. *SpringerPlus*, *5*(1), 1-11.

Hendrawan, Y., Fauzi, M. R., Khoirunnisa, N. S., Andreane, M. P. O. H., Hartianti, P. O., Halim, T. D. & Umam, C. (2019). Development of colour co-occurrence matrix (CCM) texture analysis for biosensing. In *IOP Conference Series: Earth and Environmental Science* (Vol. 230, No. 1, p. 012022). IOP Publishing.

Heng, A., Zhang, S., Tan, A. C. & Mathew, J. (2009). Rotating machinery prognostics: State of the art, challenges and opportunities. *Mechanical Systems and Signal Processing*, *23*(3), 724-739.

Horn, S., Hempel, S., Verbruggen, E., Rillig, M. C., & Caruso, T. (2017). Linking the community structure of arbuscular mycorrhizal fungi and plants: a story of interdependence? *The ISME Journal*, *11*(6), 1400-1411.

Huang, B., Zhao, B., Song, Y. (2018). Urban land-use mapping using a deep convolutional neural network with high spatial resolution multispectral remote sensing imagery. *Remote Sensing of Environment*, *214*, 73-86.

Hussain, M., Chen, D., Cheng, A., Wei, H. & Stanley, D. (2013). Change detection from remotely sensed images: From pixel-based to object-based approaches. *ISPRS Journal of Photogrammetry and Remote Sensing*, *80*, 91-106.

Kasim, A. A., Wardoyo, R. & Harjoko, A. (2017). Batik classification with artificial neural network based on texture-shape feature of main ornament. *International Journal of Intelligent Systems and Applications*, *11*(6), 55.

Lee, J., Jain, R., Khalil, K., Griffith, B., Bosca, R., Rao, G., & Rao, A. (2016). Texture feature ratios from relative CBV maps of perfusion MRI are associated with patient survival in glioblastoma. *American Journal of Neuroradiology*, *37*(1), 37-43.

Li, M., Zang, S., Zhang, B., Li, S. & Wu, C. (2014). A review of remote sensing image classification techniques: The role of spatio-contextual information. *European Journal of Remote Sensing*, *47*(1), 389-411.

Liu, N., Wan, L., Zhang, Y., Zhou, T., Huo, H. & Fang, T. (2018). Exploiting convolutional neural networks with deeply local description for remote sensing image classification. *IEEE access*, *6*, 11215-11228.

Mahmon, N. A. & Ya'acob, N. (2014). A review on classification of satellite image using Artificial Neural Network (ANN). In *2014 IEEE 5th Control and system graduate research colloquium* (pp. 153-157).

Maillard, P. (2003). Comparing texture analysis methods through classification. *Photogrammetric Engineering & Remote Sensing*, *69*(4), 357-367.

Maind, S. B. & Wankar, P. (2014). Research paper on basic of artificial neural network. *International Journal on Recent and Innovation Trends in Computing and Communication*, *2*(1), 96-100.

Maniruzzaman, M., Rahman, M., Al-MehediHasan, M., Suri, H. S., Abedin, M., El-Baz, A. & Suri, J. S. (2018). Accurate diabetes risk stratification using machine learning: role of missing value and outliers. *Journal of Medical Systems*, *42*(5), 1-17.

Mehdy, M. M., Ng, P. Y., Shair, E. F., Saleh, N., & Gomes, C. (2017). Artificial Neural Networks in Image Processing for Early Detection of Breast Cancer. *Computational and Mathematical*

Methods in Medicine, https://doi.org/10.1155/2017/2610628

Mekonnen, Y., Namuduri, S., Burton, L., Sarwat, A. & Bhansali, S. (2019). Machine learning techniques in wireless sensor network based precision agriculture. *Journal of the Electrochemical Society*, *167*(3), 037522.

Mengist, W. (2019). An Overview of the Major Vegetation Classification in Africa and the New Vegetation Classification in Ethiopia. *American Journal of Zoology*, *2*(4), 51-62.

Mocanu, D. C., Mocanu, E., Stone, P., Nguyen, P. H., Gibescu, M. & Liotta, A. (2018). Scalable training of artificial neural networks with adaptive sparse connectivity inspired by network science. *Nature Communications*, *9*(1), 1-12.

Mohammed, M. A., Abd Ghani, M. K., Hamed, R. I., Ibrahim, D. A. & Abdullah, M. K. (2017). Artificial neural networks for automatic segmentation and identification of nasopharyngeal carcinoma. *Journal of Computational Science*, *21*, 263-274.

Moshou, D., Vrindts, E., De Ketelaere, B., De Baerdemaeker, J. & Ramon, H., (2001). A neural network based plant classifier, Comput. Electron. *Agric*. 31(1), 5-16.

Murmu, S. & Biswas, S. (2015). Application of fuzzy logic and neural network in crop classification: a review. *Aquatic Procedia*, *4*, 1203-1210.

Nitze, I., Schulthess, U. & Asche, H. (2012). Comparison of machine learning algorithms random forest, artificial neural network and support vector machine to maximum likelihood for supervised crop type

classification. *Proceedings of the 4th GEOBIA, Rio de Janeiro, Brazil*, *79*, 3540.

Pang, Y., Shi, Y., Gao, S., Jiang, F., Veeranampalayam-Sivakumar, A. N., Thompson, L. & Liu, C. (2020). Improved crop row detection with deep neural network for early-season maize stand count in UAV imagery. *Computers and Electronics in Agriculture*, *178*, 105766.

Pham, M. T., Lefèvre, S., Aptoula, E. & Bruzzone, L. (2018). Recent developments from attribute profiles for remote sensing image classification. *arXiv preprint arXiv:1803.10036*.

Rashmi, S. & Mandar, S. (2011). Textural feature based image classification using artificial neural network. In *International Conference on Advances in Computing, Communication and Control* (pp. 62-69). Springer, Berlin, Heidelberg.

Salyut, J. & Kurnaz, C. (2018). Profile face recognition using local binary patterns with artificial neural network. In *2018 international conference on artificial intelligence and data processing (IDAP)* (pp. 1-4). IEEE.

Seelan, S. K., Laguette, S., Casady, G. M. & Seielstad, G. A. (2003). Remote sensing applications for precision agriculture: A learning community approach. *Remote sensing of Environment*, *88*(1-2), 157-169.

Shaha, M., & Pawar, M. (2018). Transfer learning for image classification. Proceedings of the 2nd *international conference on electronics, communication and aerospace technology (ICECA)*, pp. 656-660.

Simonthomas, S., Thulasi, N. & Asharaf, P. (2014). Automated diagnosis of glaucoma using Haralick texture features. In *International*

Conference on Information Communication and Embedded Systems (ICICES2014) (pp. 1-6).

Sootla, S, & Matiisen, T. (2015). Artificial neural network for image classification. Computational neuroscience project report submitted to the University of Tartu, 1-15.

Tehrany, M. S., Pradhan, B. & Jebuv, M. N. (2014). A comparative assessment between object and pixel-based classification approaches for land use/land cover mapping using SPOT 5 imagery. *Geocarto International*, *29*(4), 351-369.

Thai, L. H., Hai, T. S. & Thuy, N. T. (2012). Image classification using support vector machine and artificial neural network. *International Journal of Information Technology and Computer Science*, *4*(5), 32-38.

Timalsina, B., Mavoa, S. & Hahs, A. K. (2021). Dynamic Changes in Melbourne's Urban Vegetation Cover—2001 to 2016. *Land*, *10*(8), 814.

Tsai, F., (2002). A derivative-aided hyperspectral image analysis system for land-cover classification. *IEEE Trans. Geosci. Remote Sensing* 40 (2), 416-425.

Wei, Y., Zhang, X., Shi, Y., Xia, L., Pan, S., Wu, J. & Zhao, X. (2018). A review of data-driven approaches for prediction and classification of building energy consumption. *Renewable and Sustainable Energy Reviews*, *82*, 1027-1047.

Wisniewski, W. T. & Schowengerdt, R. A. (2005). Information in the joint aggregate pixel distribution of two images. In *Visual Information Processing XIV* (Vol. 5817, pp. 167-178). SPIE.

Xu, X., Li, J., Huang, X., Dalla Mura, M. & Plaza, A. (2016). Multiple morphological component analysis based decomposition for remote sensing image classification. *IEEE Transactions on Geoscience and Remote Sensing*, *54*(5), 3083-3102.

Yang, X., Tridandapani, S., Beitler, J. J., Yu, D. S., Yoshida, E. J., Curran, W. J. & Liu, T. (2012). Ultrasound GLCM texture analysis of radiation-induced parotid-gland injury in head-and-neck cancer radiotherapy: An in vivo study of late toxicity. *Medical Physics*, *39*(9), 5732-5739.

Zauner, G., Schagerl, M. & Forschungs, F. H. O. Ö. (2014). Conference 9024: Image Processing: Machine Vision Applications VII. *Electronic Imaging*, *3*, 199.

Zhang, J. & Foody, G. M., (2001). Fully-fuzzy supervised classification of sub-urban land cover from remotely sensed imagery: statistical and artificial neural network approaches. *Int. J. Remote Sensing*, 22(4), 615-628.

Zhang, Z., Wang, Z., Lin, Z. & Qi, H. (2019). Image super-resolution by neural texture transfer. In *Proceedings of the IEEE/CVF Conference on Computer Vision and Pattern Recognition* (pp. 7982-7991).

Zhao, G. & Qin, S. (2018). High-precision detection of defects of tire texture through X-ray imaging based on local inverse difference moment features. *Sensors*, *18*(8), 2524.

Zohdi, M., Rafiee, M., Kayvanfar, V. & Salamiraad, A. (2022). Demand forecasting based machine learning algorithms on customer information: an applied approach. *International Journal of Information Technology*, 1-11.